JOURNAL OF VIROLOGY, Mar. 1984, p. 947–959
0022-538X/84/030947-13$02.00/0

Vol. 49, No. 3

Transcriptional and Genetic Analyses of the Herpes Simplex Virus Type 1 Genome: Coordinates 0.29 to 0.45

LOUIS E. HOLLAND,[1] ROZANNE M. SANDRI-GOLDIN,[1]† ALAN L. GOLDIN,[1]‡ JOSEPH C. GLORIOSO,[2] AND MYRON LEVINE[1]*

Department of Human Genetics[1] and Unit for Laboratory Animal Medicine,[2] University of Michigan, Ann Arbor, Michigan 48109

Received 13 September 1983/Accepted 17 November 1983

We have constructed a map of the genes encoded by a 23,000-nucleotide-pair region of herpes simplex virus type 1. This region, defined by the three adjacent *Eco*RI fragments N (map coordinates 0.298 to 0.315), F (0.315 to 0.421), and M (0.421 to 0.448), has previously been shown by genetic analysis to contain the genes for thymidine kinase, nucleocapsid protein p40, glycoprotein B, DNA-binding protein, and DNA polymerase. We report the identification and mapping of RNAs defining 13 viral genes encoded by the region 0.298 to 0.448. The transcriptional pattern shows families of overlapping messages, similar to those observed in other regions of the viral genome. We also isolated mutants representing four distinct complementation groups and physically mapped several of the mutations to regions within *Eco*RI fragment F by marker rescue. Mutations representing complementation groups 1-9 (glycoprotein B), 1-1 (DNA-binding protein), and 1-3 (DNA polymerase) were mapped to coordinates 0.361 to 0.368, 0.386 to 0.411, and 0.411 to 0.421, respectively. A fourth previously undefined complementation group was mapped to the region between glycoprotein B and DNA-binding protein. Comparing the transcription mapping with marker rescue data suggests that the genes for glycoprotein B, DNA-binding protein, DNA polymerase, and nucleocapsid protein p40 are expressed as 3.3-, 4.2-, 4.3- or 4.2- or both, and 2.4-kilobase mRNAs, respectively.

Functions are known for relatively few of the 50 or more viral polypeptides synthesized during herpes simplex virus type 1 (HSV-1) infection (57). However, several of the viral genes for which functions are known are located in a region near the center of the long unique segment of the HSV-1 genome. This region, located between map coordinates 0.29 and 0.45 relative to the prototype orientation, contains the thymidine kinase (TK) gene near the left end (34, 63, 69), the DNA polymerase gene near the right end (7–9, 12, 13, 27), and genes for a capsid protein (42), glycoprotein B (14, 23, 30), and the major DNA-binding protein (10, 29, 67) in between. This region is thought to also contain an origin for viral DNA replication (16, 55) and has been associated with morphological transformation (5, 47).

We have recently constructed cell lines containing stably integrated viral sequences representing coordinates 0.315 to 0.421 of the HSV-1 genome (48). We demonstrated functional expression of four viral genes encoded within this region by complementation of infecting HSV-1 temperature-sensitive (*ts*) mutants. Although the level of constitutive expression of the viral genes resident in the cell lines was very low, the functional expression of at least two of these genes (glycoprotein B and DNA-binding protein) was induced by a transacting α gene product (ICP4) synthesized from the infecting virus genome.

A better understanding of the regulation of viral genes encoded between coordinates 0.29 and 0.45 is dependent on the availability of a detailed map of these genes. *Eco*RI fragment F (0.315 to 0.421) and the two adjacent *Eco*RI fragments, N (0.298 to 0.315) and M (0.421 to 0.448) (19), provided the tools necessary for constructing such a map. As a further aid in this construction, a detailed restriction map was made, and several subclones were isolated from this region.

We took two approaches to characterizing the viral genes encoded within the region 0.29 to 0.45. The first approach was to isolate mutants in several complementation groups and then define their location by marker rescue. The mapping of mutations in four distinct complementation groups to regions within *Eco*RI-F (0.315 to 0.421) is presented here. Preston et al. (42) have identified a mutant which defines a fifth complementation group in this region. Complementation groups have also recently been mapped to the adjacent regions, *Eco*RI-N (0.298 to 0.315) (66) and *Eco*RI-M (0.421 to 0.448) (9).

The second approach was to map the mRNAs transcribed between coordinates 0.29 and 0.45. This identified nine viral genes either partially or completely encoded within *Eco*RI fragment F (0.315 to 0.421). The early mRNA mapping studies of Anderson et al. (2) and Holland et al. (21) identified major viral transcripts of 4.3, 3.3, and 1.5 kilobases (kb) from this region. Similar transcripts are reported here, and their precise locations are established. We also identify transcripts defining four additional viral genes in the adjacent regions. Two of these confirm the results of Sharp et al. (51). From our study we are able to make several correlations relating specific viral transcripts to defined complementation groups.

MATERIALS AND METHODS

Cells and viruses. Primary rabbit kidney cells and Vero cells were maintained in Eagle minimum essential medium containing Hanks salts (GIBCO Laboratories) and supplemented with tryptose phosphate broth, nonessential amino acids, 10% heat-inactivated fetal calf serum (GIBCO), 100 μg of streptomycin per ml, and 100 U of penicillin per ml.

* Corresponding author.
† Present address: Department of Microbiology, University of California, Irvine, CA 92717.
‡ Present address: Department of Chemistry, California Institute of Technology, Pasadena, CA 91125.

KB cells were maintained in medium which was similarly supplemented but contained 10 mM HEPES (*N*-2-hydroxyethylpiperazine-*N'*-2-ethanesulfonic acid) (pH 7.15) and 10% newborn calf serum (Biocell Laboratories) instead of the heat-inactivated fetal calf serum.

The isolation procedure for the *ts* mutants used in this study (see Table 2) has been previously described (18, 49). Stocks of HSV-1 strain KOS 1.1 and *ts* mutant viruses were grown by infection of Vero cells at low multiplicity and titrated by plaque assay on Vero cells. Strain KOS stocks were grown at 37°C; *ts* mutant stocks were grown at 34°C.

Isolation of viral DNA. Viral DNA was purified from HSV-1 (KOS)- and *ts* mutant-infected Vero cell lysates by CsCl density gradient centrifugation (49).

Restriction endonuclease mapping. Restriction endonucleases were obtained from Bethesda Research Laboratories; digestions were performed by following their specifications. Previously unmapped restriction endonuclease sites were identified from series of single and multiple enzyme digestions of plasmids pSG18 (*Eco*RI-F, 0.315 to 0.421) and pSG17 (*Eco*RI-M, 0.421 to 0.448) (19). Products of the digestions were separated by electrophoresis in 0.7 or 1% agarose gels and visualized by UV fluorescence of ethidium bromide-stained DNA (19, 49). Restriction fragment sizes were determined based on their migration relative to fragments of known size from λ DNA digests. The size of fragments less than 1,000 base pairs (bp) in length was determined by electrophoretic migration in 5% polyacrylamide gels (32) relative to size standards obtained from pBR322 digestion. A composite map of the restriction endonuclease recognition sites is presented in Fig. 1.

During the restriction endonuclease mapping, we discovered that two forms of pSG18 existed, each having a small deletion relative to wild-type DNA near the right end of the *Eco*RI-F fragment. *Bam*HI digestion yielded a 2,300-bp fragment from one population of pSG18, a 2,200-bp fragment from the other pSG18 population, and a 2,400-bp fragment from HSV-1 (KOS) virion DNA. The sizes shown for the restriction fragments in Fig. 1 reflect the sizes obtained from digestion of the pSG18 containing the smaller deletion. Post et al. (40) reported the inability to clone the wild-type *Bam*HI fragment from the region in which we detect deletions. Spaete and Frenkel (55) and Weller et al. (67) have also reported the observation of deletions occurring in all clones spanning the region of this *Bam*HI fragment.

Construction of chimeric plasmids. The *Pst*I, *Eco*RI, *Bam*HI, and *Sal*I cloning sites in vectors pBR322 and pBR325 were used individually and in combination for generating subclones from pSG18 and pSG17. Vector pBR322 DNA, digested and then tailed at the *Pst*I site with dGMP, was annealed with an *Sst*I-digested and then dCMP-tailed sample of pSG18 DNA to produce the recombinant plasmids containing *Sst*I fragments (61). Procedures for ligation and transformation into *Escherichia coli* K-12 DH-1 have been described previously (19). The cloned fragments were identified by a rapid lysis extraction of the plasmid DNA (24), followed by appropriate restriction endonuclease digestion and agarose gel electrophoresis (19). The restriction fragments which were cloned are indicated in Fig. 1 and listed in Table 1.

Subclone nomenclature consists of the plasmid of origin (pSG18 or pSG17), followed by a letter designation identifying the restriction sites at the fragment ends (B for *Bam*HI, E for *Eco*RI, P for *Pst*I, S for *Sal*I, and St for *Sst*I) and a number relating to the cloned isolate. Plasmids referred to as pLH-50, pHV-4, pHV-5, and pHV-11 in Holland et al. (23) are now designated pSG18-B50, pSG18-St4, pSG18-St5, and pSG18-St11, respectively.

Plasmid DNA extraction. Plasmid DNA was isolated from 1 liter of bacterial cultures by using the Holmes and Quigley lysis-by-boiling method (24) as described by Maniatis et al. (31), followed by banding in a cesium chloride-ethidium bromide gradient.

Complementation tests. The *ts* mutants were complemented with each other by a procedure similar to the quantitative complementation test of Schaffer et al. (50) as described previously (18).

Measurement of DNA synthesis. Viral DNA synthesis was assayed by CsCl gradient fractionation of the DNA isolated from infected cells which were labeled with 10 μCi of [*methyl*-^{3}H]thymidine per ml from 4 to 24 h postinfection as previously described (49).

Measurement of DNA polymerase activity. Viral DNA polymerase activity was assayed by the method of Weissbach et al. (64) as described previously (1).

Marker rescue analysis. Transfections for mapping mutations by marker rescue were performed by using a modification of the method of Wigler et al. (68) as described previously (19).

Isolation of viral RNA. KB cells, grown in T-150 flasks (Corning), were infected at a multiplicity of 10 PFU per cell for 30 min at 37°C with an inoculum of 6 ml per flask. The cells were pulse labeled with 5 to 10 μCi of [^{3}H]uridine (New England Nuclear Corp.) per ml for 60 min just before extraction. For the drug inhibition study, cells were maintained in medium containing 1.9×10^{-4} M 1-β-D-arabinofuranosylthymine (Sigma Chemical Co.) continuously from 1 h before infection until extraction. Time after infection was measured from the start of absorption.

Polyribosome-associated RNA was isolated from cells lysed with Triton X-100 (Sigma Chemical Co.) by using the Mg^{2+} precipitation method of Palmiter (37), followed by proteinase K (Boehringer Mannheim) digestion and phenol-chloroform extraction (58). The polyadenylated RNA was purified by using oligodeoxythymidylic acid-cellulose (Collaborative Research, Inc.).

Size fractionation and hybridization analysis of RNA. Polyadenylated RNA, isolated as described above, was denatured by glyoxalation and size fractionated by electrophoresis in horizontal 1% agarose gels (6, 35). The RNA was then transferred to nitrocellulose paper (BA-85; Schleicher and Schuell) by using 20× SSC (1× SSC is 0.15 M NaCl plus 0.015 M sodium citrate) as described by Southern (54) and Thomas (60). RNA blots were prehybridized for 18 h at 42°C in buffer containing 50% formamide, 5× SSC, 50 mM sodium phosphate buffer at pH 6.5, sonicated denatured salmon sperm DNA at 250 μg/ml, 0.02% each of bovine serum albumin, Ficoll, and polyvinylpyrrolidone, and 0.05% sodium dodecyl sulfate (60). Hybridizations were for 24 h at 42°C in a solution containing four parts of the buffer used for prehybridization and one part 50% dextran sulfate (60). Probes were ^{32}P-labeled by nick translation (19), denatured at 117°C for 7 min, cooled, and added to the hybridization solution at a concentration of 5×10^5 cpm/ml. After hybridization, the RNA blots were washed four times for 5 min each time at room temperature in 2× SSC–0.1% sodium dodecyl sulfate and then washed two times for 20 min each time at 50°C in 0.1× SSC–0.1% sodium dodecyl sulfate (60). The nitrocellulose strips were wrapped in Saran Wrap and exposed to Kodak X-Omat AR film.

RNA blots were stripped for rehybridization by a modification of the method described by Thomas (60). Two 1-h

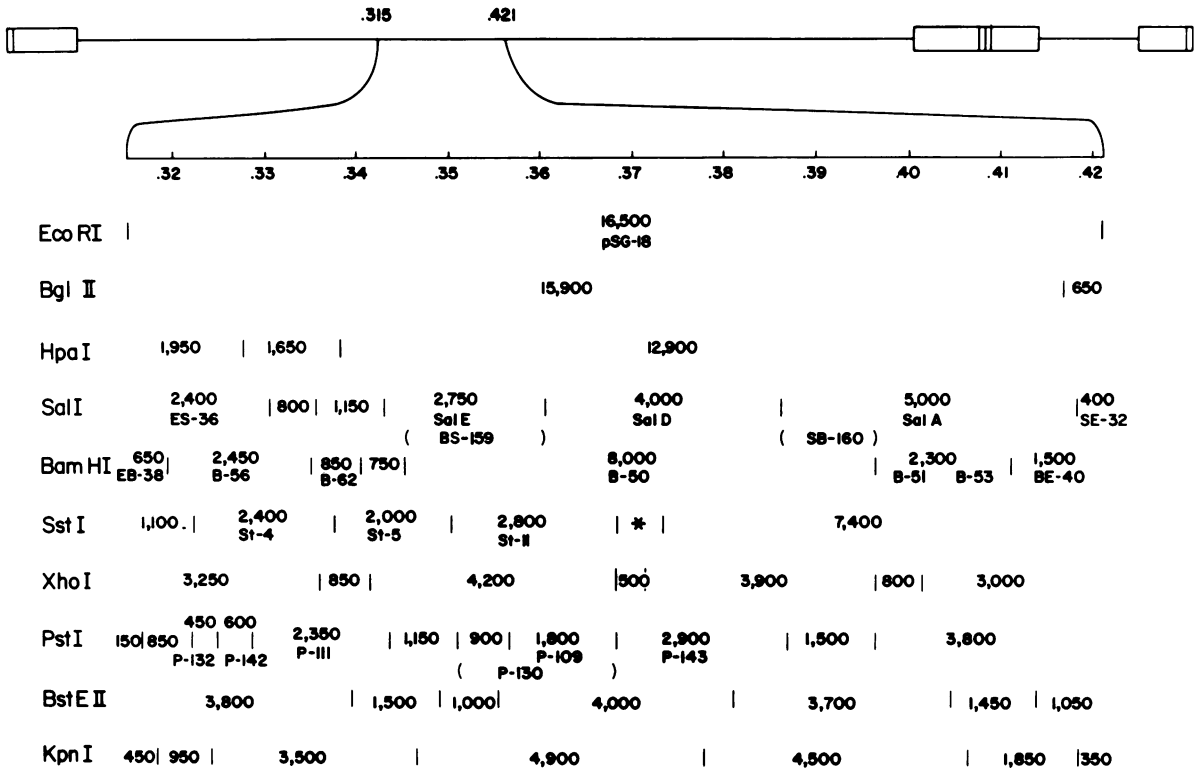

FIG. 1. Map of restriction endonuclease fragments and subclones within the *Eco*RI fragment F region. The relative position and map coordinates for *Eco*RI fragment F in the prototype arrangement of HSV-1 (KOS) is shown at the top. Also shown are the sizes in nucleotide pairs and the relative positions for the fragments generated from cleavage of pSG-18 (19) with the restriction endonucleases indicated on the left. An abbreviated designation for a fragment subclone is shown below the size for that fragment. Complete designations and map coordinates for the clones are shown in Table 1. Clone BS-159 contains the 2,400-bp region between the indicated *Bam*HI and *Sal*I sites; clone SB-160 contains the 1,600-bp region between the indicated *Sal*I and *Bam*HI sites; clone P-130 contains both the 900- and 1,800-bp *Pst*I fragments. The asterisk located near coordinate 0.37 in the *Sst*I map represents an 800-bp region containing at least three additional *Sst*I cleavage sites.

washes at 80°C were performed in buffer containing 50% formamide and 0.05× wash buffer (1× wash buffer contains 50 mM Tris-hydrochloride at pH 8.0, 2 mM EDTA, 0.5% sodium pyrophosphate, 0.02% each of bovine serum albumin, Ficoll, and polyvinylpyrrolidone, and 1% sodium dodecyl sulfate), followed by a 5-min wash at room temperature in 0.05× wash buffer in the absence of formamide. RNA blots could be cycled through at least three rounds of hybridization without detectable changes in efficiency or specificity.

RNA size determination. The sizes of the hybridizing transcripts were determined by their migration relative to size standards electrophoresed in adjacent lanes. Two types of size standard were used. KB cells were grown in medium containing 100 μCi of [$^{32}P_i$] per ml for 24 h. The labeled RNA extracted from the polyribosomes consisted primarily of the 28S and 18S (5.2 and 2.0 kb, respectively) (35, 65) rRNAs. Approximately 25,000 cpm of this RNA, glyoxalated in parallel and electrophoresed in lanes adjacent to the infected cell RNA samples, served both as size markers and a means of monitoring the efficiency of transfer to nitrocellulose (routinely greater than 90%).

The second type of size standard consisted of single-stranded DNA. The products of three separate digests of pBR325 (41) were mixed together, providing five different size restriction fragments. A 5,995-bp fragment was obtained from linearizing pBR325 with *Eco*RI; pBR325 cut with *Eco*RI and *Bam*HI provided fragments of 4,403 and 1,592 bp, and pBR325 cut with *Pst*I and *Hin*dIII provided 3,583- and 2,412-bp fragments (41, 59). A mixture of these fragments was denatured by glyoxalation, electrophoresed, and transferred along with the ^{32}P-labeled rRNA. When chimeric plasmids containing fragments of HSV-1 DNA inserted into either pBR322 or pBR325 were labeled by nick translation and used as hybridization probes, the ^{32}P-labeled HSV sequences hybridized to specific viral mRNA species, and the ^{32}P-labeled pBR322 or pBR325 sequences hybridized to the five pBR325 fragments in the adjacent slot. Single-stranded RNA and single-stranded DNA have been shown to migrate similarly in agarose gels after glyoxalation (6, 35). When the logarithm of the fragment size in nucleotides was plotted against mobility for our five DNA and two RNA size markers, a straight line could be drawn through all seven points. This provided a standard curve for molecules ranging in size from 6 to 1.6 kb. Subsequently, the ^{32}P-labeled rRNA was discontinued as a size marker, and the single-stranded DNA markers were expanded to provide a size range from 10 to 1.1 kb.

M13 cloning. Restriction fragments were cloned into the replicative form of the single-stranded DNA phage M13*mp*8 (36). Phage stocks were grown from the colorless plaques resulting from transformation of *E. coli* JM103. The nature of the recombinants was confirmed by restriction endonuclease analysis of the phage replicative-form DNA.

M13 hybridization probes. A method similar to that described by Hu and Messing (25) was used for making strand-

TABLE 1. Genomic locations of plasmid inserts

Plasmid name	Vector	Map coordinates[a]	Termini[b]
pSG87 (*Eco*RI-N)[c]	pBR325	0.298–0.315	*Eco*RI-*Eco*RI
pSG18 (*Eco*RI-F)[c]	pBR325	0.315–0.421	*Eco*RI-*Eco*RI
pSG18-ES36	pBR325	0.315–0.331	*Eco*RI-*Sal*I
pSG18-*Sal*I E[d]	pBR325	0.343–0.361	*Sal*I-*Sal*I
pSG18-*Sal*I D[d]	pBR325	0.361–0.386	*Sal*I–*Sal*I
pSG18-*Sal*I A[d]	pBR325	0.386–0.418	*Sal*I-*Sal*I
pSG18-SE32	pBR325	0.418–0.421	*Sal*I-*Eco*RI
pSG18-EB38	pBR325	0.315–0.320	*Eco*RI-*Bam*HI
pSG18-B56	pBR322	0.320–0.335	*Bam*HI-*Bam*HI
pSG18-B62	pBR322	0.335–0.341	*Bam*HI-*Bam*HI
pSG18-B50	pBR322	0.346–0.397	*Bam*HI-*Bam*HI
pSG18-B50-BS159	pBR322	0.346–0.361	*Bam*HI-*Sal*I
pSG18-B50-SB160	pBR322	0.386–0.397	*Sal*I-*Bam*HI
pSG18-B51[e]	pBR322	0.397–0.411	*Bam*HI-*Bam*HI
pSG18-B53[e]	pBR322	0.397–0.411	*Bam*HI-*Bam*HI
pSG18-BE40	pBR325	0.411–0.421	*Bam*HI-*Eco*RI
pSG18-St4	pBR322	0.322–0.338	*Sst*I-*Sst*I[f]
pSG18-St5	pBR322	0.338–0.351	*Sst*I-*Sst*I[f]
pSG18-St11	pBR322	0.351–0.368	*Sst*I-*Sst*I[f]
pSG18-P132	pBR322	0.322–0.325	*Pst*I-*Pst*I
pSG18-P142	pBR322	0.325–0.329	*Pst*I-*Pst*I
pSG18-P111	pBR322	0.329–0.344	*Pst*I-*Pst*I
pSG18-P130	pBR322	0.351–0.368	*Pst*I-*Pst*I
pSG18-P109	pBR322	0.357–0.368	*Pst*I-*Pst*I
pSG18-P143	pBR322	0.368–0.387	*Pst*I-*Pst*I
pSG17 (*Eco*RI-M)[c]	pBR325	0.421–0.448	*Eco*RI-*Eco*RI
pSG17-EB71	pBR325	0.421–0.434	*Eco*RI-*Bam*HI

[a] The coordinates represent the map position in the prototype arrangement for the restriction site at the left and right end of the fragment cloned.

[b] The restriction endonuclease sites defining the left and right ends of the cloned fragments are indicated.

[c] See Goldin et al. (19).

[d] Obtained from D. Knipe (29).

[e] pSG18-B51 contains a 2,300-bp *Bam*HI fragment; pSG18-B53 contains a 2,200-bp *Bam*HI fragment. Both clones contain deletions relative to the genomic *Bam*HI fragment.

[f] Cloned into the *Pst*I site.

specific hybridization probes. An annealing mixture containing 5 μl of template (100 to 400 ng), 2 μl of a 16-base hybridization probe primer (35 ng; New England Biolabs), 2 μl of 10× reaction buffer (10× buffer is 500 mM NaCl, 100 mM Tris-hydrochloride [pH 7.5], 100 mM dithiothreitol, 100 mM $MgCl_2$), and 1 μl of water was sealed in a capillary tube, placed in boiling water for 3 min, and allowed to cool to room temperature for 30 min. The annealed primer-template solution was then added to a 1.5-ml microcentrifuge tube containing 10 μl of 50 μM dATP, dTTP, and dGTP, 2.5 μM dCTP, and 30 to 50 μCi of [α-^{32}P]dCTP (800 Ci/mmol; New England Nuclear). The amount of the labeled triphosphate was limiting so that synthesis was contained to the M13 vector sequences and did not continue through the insert. *E. coli* DNA polymerase I (large fragment, 4 U in 0.5 μl; New England Nuclear) was added, and the reaction was allowed to proceed at room temperature for 45 min. The reaction was stopped by adding 1 μl of 0.5 M EDTA (pH 7.8) and 10 μg of tRNA carrier and adjusting the volume to ca. 0.2 ml by adding 180 μl of 10 mM Tris-hydrochloride (pH 7.8)–1 mM EDTA. Samples were then extracted once with an equal volume of recrystallized phenol (saturated with 1 M Tris-hydrochloride [pH 8.0] and containing 0.1% 8-hydroxyquinoline). The aqueous phase was added to an equal volume of 4 M ammonium acetate, pH 7.4, and precipitated by adding 2 volumes of cold absolute ethanol. The precipitate was collected by a 5-min spin at 16,500 × *g* in a microcentrifuge and resuspended in 50 μl of 10 mM Tris-hydrochloride (pH 7.8)–1 mM EDTA. These probes were then used in hybridizations to RNA blots at a concentration of 3×10^5 cpm/ml as described above, being careful not to denature the labeled DNA.

RESULTS

Grouping and characterization of mutants. A series of pairwise complementation tests involving all of the mutants listed in Table 2 were performed. These mutants could be placed into four distinct complementation groups based on the complementation indices. The complementation index was defined as the titer of the mixed infection divided by the sum of the titers of each mutant. Paired mutant infections from within a group had a complementation index of 1 or less; paired mutant infections from between groups had a complementation index of 10 or greater. Mutants were assigned to standard complementation group 1-1, 1-3, or 1-9 based on their failure to complement mutants *ts*656, *ts*833, or *ts*822, respectively (50). Two of the mutants, *ts*8 and *ts*17, complemented the mutants in groups 1-1, 1-3, and 1-9 as well as mutants in other defined complementation groups, thereby defining a new complementation group. Mutant 17*tsVP*1201 (42) complemented all of our mutants, and therefore represented another new complementation group (data not shown). Mutants from each group were characterized by their ability to synthesize viral DNA (49) and by their DNA polymerase activity (1) at the nonpermissive temperature. These results are summarized in Table 2.

Mapping of *ts* mutations by marker rescue. Several of the mutants were further characterized by cotransfection mark-

TABLE 2. Summary of genetic information

Complementation group	Mutant[a]	Nature of mutagenesis[b]	DNA synthesis	DNA Pol	Marker rescue coordinates	Function
1-1	*ts*4	BUdR	−		0.386–0.397	DNA-binding protein
	*ts*6	BUdR	−			
	*ts*13	BUdR				
	*ts*14	BUdR	−			
	*ts*18	BUdR	−	+	0.397–0.411	
	*ts*62	NA[f]			0.397–0.411	
	*ts*88	NA[f]			0.386–0.418	
	*ts*B84	NA[f]	−		0.397–0.411	
	*ts*656[d]	BUdR	−			
1-3	*ts*16	BUdR	−	−	0.411–0.418	DNA polymerase
	*ts*833[d]	BUdR	−		0.411–0.421	
1-9	*ts*2	BUdR				
	*ts*B5[e]	BUdR	+		0.361–0.368[g]	Glycoprotein B
	*ts*822[d]	BUdR	+	+		
ND[c]	*ts*8	BUdR	+	+	0.378–0.397	Unknown
	*ts*17	BUdR	+		0.315–0.421	

[a] Unless otherwise indicated, mutants were isolated in our laboratory from the KOS 1.1 strain of HSV-1 (18, 49).
[b] Mutagenesis was performed in vivo by using the indicated agent, unless stated otherwise. NA is nitrous acid; BUdR is 5-bromo-2'-deoxyuridine.
[c] ND, Not defined.
[d] Mutant was obtained from Hughes and Munyon; parental strain was KOS 1.1 (26).
[e] Mutant was obtained from A. Buchan; parental strain was HFEM (33).
[f] Mutagenesis was performed in vitro (49).
[g] Data from Holland et al. (23).

er rescue experiments. Mutations initially mapped to the *Eco*RI-F fragment (map coordinates 0.315 to 0.421) were more precisely mapped in experiments with subcloned regions of that fragment (Fig. 1 and Table 1). Percent rescue, defined as 100 times the titer at 39°C divided by the titer at 34°C, was considered significant when it was greater than 1%. This percentage of rescue was at least 10-fold above the background level for each mutant.

The limits for marker rescue mapping of mutations in each complementation group are summarized in Table 2 and shown in Fig. 4. Five mutants in complementation group 1-1 were used in mapping studies. All were rescued by plasmid pSG18-*Sal*I-A, which contains the *Sal*I fragment between coordinates 0.386 and 0.418. Four of these mutations were mapped more precisely within that region. Mutant *ts*4 was rescued with the plasmid pSG18-B50 (0.346 to 0.397) in addition to pSG18-*Sal*I-A. The region common to these two plasmids is the region between the *Sal*I site at 0.386 and the *Bam*HI site at 0.397. Mutants *ts*18, *ts*62, and *tsB*84 were rescued with plasmid pSG18-B53 (0.397 to 0.411), but they were not rescued with pSG18-B50, mapping the site for these three mutations to the right of the *ts*4 mutation. Thus, marker rescue analysis allowed us to distinguish mutations within complementation group 1-1 based on their physical location. Similar results defining two regions of *ts* lesions for group 1-1 mutants have been reported by Weller et al. (67).

Two mutants in complementation group 1-3 were rescued with plasmid pSG18-EB40 (0.411 to 0.421). Mutant *ts*16 was also rescued by the plasmid pSG18-*Sal*I-A, thereby narrowing the site of this mutation to the 1,100-bp region between the *Bam*HI site at 0.411 and the *Sal*I site at 0.418. Other mutations in complementation group 1-3 have also been mapped to this region (7, 9).

Mutant *ts*B5 in complementation group 1-9 was rescued with plasmids pSG18-St11 (map coordinates 0.351 to 0.368) and pSG18-*Sal*I-D (0.361 to 0.386), positioning the site of this mutation to the 1,200-bp region between the *Sal*I site at 0.361 and the *Sst*I site at 0.368 (23). DeLuca et al. have also shown the *ts* lesion of mutant *tsB5* to map to this region (14).

Mutants *ts*8 and *ts*17 represent a complementation group which has not been correlated with the groups of Schaffer et al. (50). Although these mutations have been more difficult to map by marker rescue, they have both been rescued by the cloned *Eco*RI fragment F (pSG18, 0.315 to 0.421). Mutant *ts*8 also rescued with plasmid pSG18-B50 (0.346 to 0.397) and a gel-purified 4,500 bp *Kpn*I fragment (0.378 to 0.407). This maps location of the mutation to the 3,000-bp region between the *Kpn*I site at 0.378 and the *Bam*HI site at 0.397.

Northern hybridization analysis. Polyadenylated RNA was isolated from the polyribosomes of HSV-1-infected cells at 6.5 h postinfection. The RNA was denatured by glyoxalation, size fractionated by agarose gel electrophoresis, and then transferred to nitrocellulose paper for use in hybridization reactions. Adjacent, as well as overlapping, restriction fragment subclones and gel-purified restriction fragments from the *Eco*RI fragments N (0.298 to 0.315), F (0.315 to 0.421), and M (0.421 to 0.448) were labeled in vitro with ^{32}P by nick translation and used as hybridization probes.

Five mRNAs which were found to be overlapping and aligned at one end were mapped to the region 0.309 to 0.351. Plasmid pSG18-EB38, which contains HSV-1 DNA representing map coordinates 0.315 to 0.320, hybridized to RNA 5.6 and 5.2 kb in size (Fig. 2, lane 6). When the adjacent 900-bp *Hin*fI-*Eco*RI fragment (0.309 to 0.315), gel purified from a *Hin*fI-*Eco*RI digestion of pSG87, was used as the probe, hybridization was seen to the 5.6-kb mRNA but not the 5.2-kb mRNA (Fig. 2, lane 4). This indicated that the 5.6-kb mRNA spans the *Eco*RI site at 0.315 and that the 5.2-kb mRNA does not. This probe also hybridized to the expected

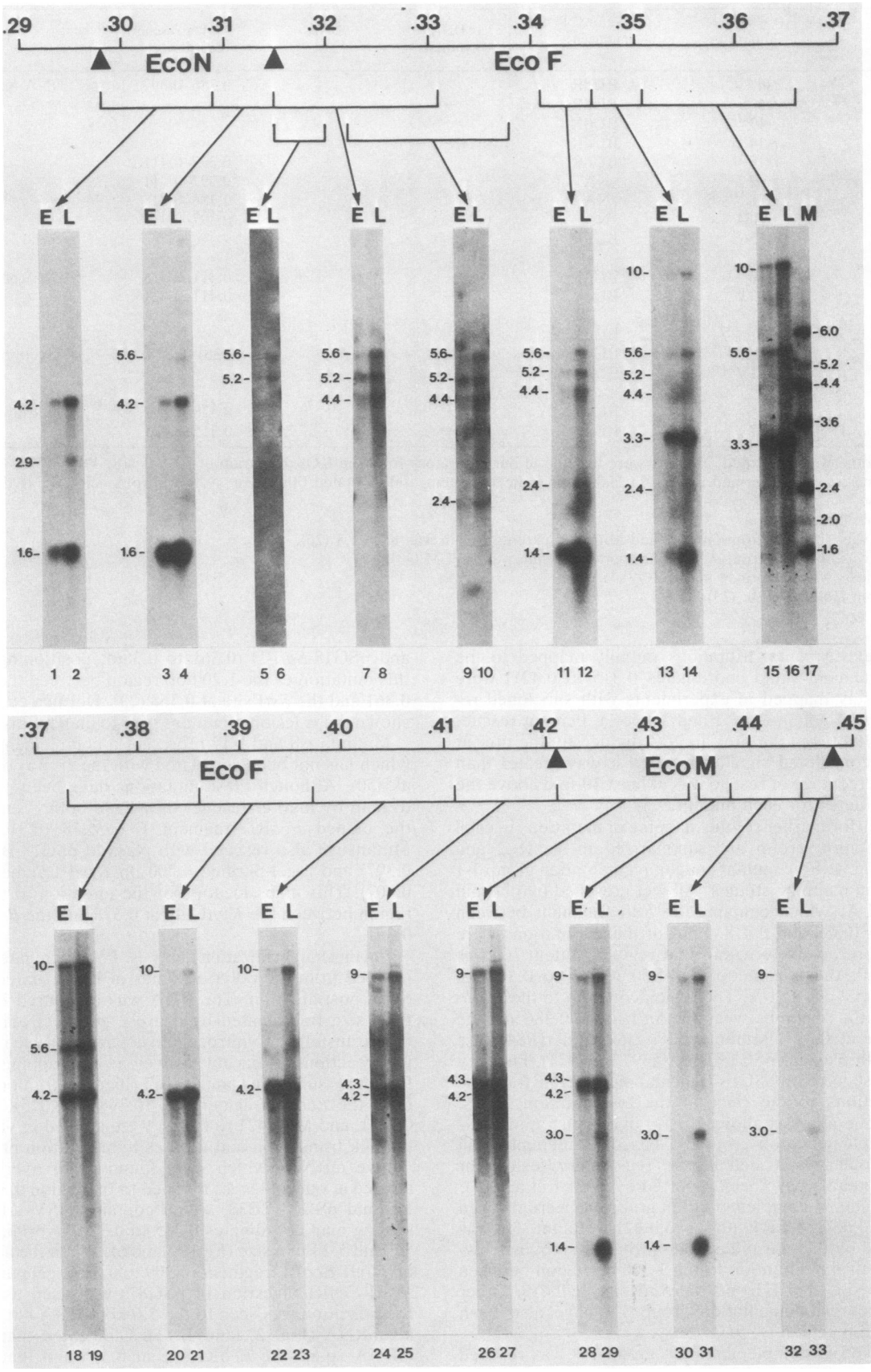
.29
.30
.31
.32
.33
.34
.35
.36
.37
EcoN
Eco F
E L
E L M
1 2
3 4
5 6
7 8
9 10
11 12
13 14
15 16 17
.37
.38
.39
.40
.41
.42
.43
.44
.45
Eco F
Eco M
18 19
20 21
22 23
24 25
26 27
28 29
30 31
32 33

TABLE 3. Strand-specific M13 clones

Clone designation	Parental plasmid[a]	Fragment[b]	Coordinates[c]	Strand[d]	Hybridizing[e] RNA (kb)
BS-21	pSG18-B56	*Bam*HI-*Sal*I	0.320–0.331	*l*	
BS-22	pSG18-B56	*Sal*I-*Bam*HI	0.331–0.335	*r*	5.6,5.2,4.4,2.4
S-3	pSG18-P111	*Sal*I-*Sal*I	0.336–0.343	*r*	5.6,5.2,4.4,2.4,1.4
B-5	pSG18-St5	*Bam*HI-*Bam*HI	0.341–0.346	*r*	5.6,5.2,4.4,2.4,1.4
B-6	pSG18-St5	*Bam*HI-*Bam*HI	0.341–0.346	*l*	
SP-2	pSG18-P109	*Pst*I-*Sal*I	0.357–0.361	*r*	
SP-4	pSG18-P109	*Sal*I-*Pst*I	0.361–0.368	*l*	10,5.6,3.3
BS-9	pSG18-B53	*Bam*HI-*Xho*I[f]	0.397–0.402	*l*	10,4.2
BS-8	pSG18-B53	*Xho*I-*Bam*HI[f]	0.402–0.411	*r*	
BS-4	pSG18-BE40	*Bam*HI-*Sal*I	0.411–0.418	*l*	
EB-1	pSG18-BE40	*Bam*HI-*Eco*RI	0.411–0.421	*r*	9,4.3,4.2

[a] Listed is the plasmid clone which was digested to provide the restriction fragment for cloning into M13*mp*8 (see Fig. 1 and Table 1).
[b] Restriction endonuclease sites, which define the left and right ends of the fragment cloned into M13*mp*8, are indicated.
[c] The coordinates represent the map positions in the prototype arrangement for the restriction sites at the left and right ends of the cloned fragment.
[d] The polarity of the viral strand contained in the single-stranded phage clone is indicated. The *r* strand is defined as the strand transcribed in the rightward direction; the *l* strand is transcribed in the leftward direction.
[e] Summarized from Fig. 3.
[f] This fragment was cloned into M13*mp*8 cut at the *Bam*HI and *Sal*I sites.

1.6-kb TK gene transcript (11, 51) and a larger TK-related transcript of 4.2 kb. The 1.6- and 4.2-kb mRNAs as well as a 2.9-kb mRNA, but not the 5.6-kb mRNA, hybridized to a 1,500-bp *Eco*RI-*Hin*fI fragment (0.298 to 0.309) gel purified from a *Hin*fI-*Eco*RI digestion of pSG87, which extends further to the left in the prototype arrangement of HSV-1 (Fig. 2, lane 2).

In addition to the 5.6- and 5.2-kb mRNAs which hybridized to plasmid pSG18-EB38 (0.315 to 0.320; Fig. 2, lane 6), plasmid pSG18-ES36, containing viral sequences from the region 0.315 to 0.331, hybridized to RNA 4.4 kb in size (Fig. 2, lane 8). The viral fragment in plasmid pSG18-St4 (0.322 to 0.338), which partially overlaps the fragment in plasmid pSG18-ES36, hybridized to the 5.6-, 5.2-, and 4.4-kb mRNAs in addition to RNA 2.4 kb in size (Fig. 2, lane 10). A 750-bp *Bam*HI fragment (0.341 to 0.346), gel purified from a *Bam*HI digest of pSG18-St5, hybridized to a 1.4-kb mRNA in addition to the four mRNAs seen hybridizing with the previous fragment (Fig. 2, lane 12). These five overlapping mRNAs also hybridized to the adjacent 800-bp *Bam*HI-*Sst*I fragment (map coordinates 0.346 to 0.351), gel purified from a *Bam*HI-*Sst*I digestion of pSG18-*Sal*I-E, (Fig. 2, lane 14), but did not hybridize to viral sequences in plasmid pSG18-St11 (0.351 to 0.368; Fig. 2, lane 16). This indicated that their transcription spans the *Bam*HI site at 0.346 but not the *Sst*I site at 0.351. The 5.6-kb RNA which hybridized to pSG18-St11 represents a second message, equivalent in size to the one described above, but mapping to the right of it (see below).

Plasmid pSG18-St11 (0.351 to 0.368) hybridized to mRNA of 10, 5.6, and 3.3 kb (Fig. 2, lane 16). The 2,000-bp *Sst*I-*Sal*I fragment (0.373 to 0.386), gel purified from an *Sst*I-*Sal*I digestion of pSG18-*Sal*I-D, hybridized to the 10- and 5.6-kb mRNAs and to a 4.2-kb mRNA (Fig. 2, lane 19). Plasmid pSG18-B50-SB160 (0.386 to 0.397) and plasmid pSG18-B53 (0.397 to 0.411) hybridized to only the 10- and 4.2-kb mRNAs (Fig. 2, lanes 21 and 23). The 3.3-kb mRNA spanned at its left end the *Sst*I site at 0.351 (Fig. 2, lanes 14 and 16) but not the *Bam*HI site at 0.346 (Fig. 2, lanes 12 and 14). At its right end this message spanned the *Pst*I site at 0.367 (data not shown) but not the *Sst*I site at 0.373 (Fig. 2, lane 19). All probes between the *Bam*HI site at 0.346 and the *Bam*HI site at 0.411, a region of 10,300 bp, hybridized to the 10-kb transcript (Fig. 2, lanes 14, 16, 19, 21, and 23). The left end of this transcript spanned the *Sst*I site at 0.351 (Fig. 2, lanes 14 and 16) but not the *Bam*HI site at 0.346 (lanes 12 and 14); its right end did not span the *Bam*HI site at 0.411 (lanes 23 and 25) but did span the *Kpn*I site at 0.407 (data not shown). The left end of the 4.2-kb mRNA was transcribed across the *Sal*I site at 0.386 (Fig. 2, lanes 19 and 21) but did not span the *Bst*EII site at 0.381 (data not shown). The right end of this transcript extended across the *Kpn*I site at 0.407 (data not shown); that it did not span the *Bam*HI site at 0.411 was shown by use of strand-specific hybridization probes (see below). The 5.6-kb mRNA spanned the *Sst*I site at 0.351 (Fig. 2, lanes 14 and 16) at its left end and a *Bst*EII site at 0.381 (data not shown) at its right end, but it did not span the *Sal*I site at 0.386 (lanes 19 and 21).

The 5.6-kb mRNA mapping between 0.346 and 0.386 could not be distinguished from the 5.6-kb mRNA mapping be-

FIG. 2. Northern hybridization analysis of mRNA encoded in the region 0.298 to 0.448. Polyadenylated RNA was isolated at 6.5 h postinfection from the polyribosomes of cells maintained either in medium containing 1.9×10^{-4} M 1-β-D-arabinofuranosylthymine (odd-numbered lanes 1 through 15 and even-numbered lanes 18 through 32, labeled E) or in drug-free medium (even-numbered lanes 2 through 16 and odd-numbered lanes 19 through 33, labeled L). Map coordinates relative to the prototype arrangement of HSV-1 and the positions of *Eco*RI cleavage sites within the region 0.29 to 0.45 are indicated. The relative position of each fragment used as a probe is shown along with its corresponding hybridization pattern. The sizes of the hybridizing transcripts are given in kilobases. Hybridization results are shown for the following probes: *Eco*RI-*Hin*fI fragment, coordinates 0.298 to 0.309 (lanes 1 and 2); *Hin*fI-*Eco*RI fragment, 0.309 to 0.315 (lanes 3 and 4); pSG18-EB38, 0.315 to 0.320 (lanes 5 and 6); pSG18-ES36, 0.315 to 0.331 (lanes 7 and 8); pSG18-St4, 0.322 to 0.338 (lanes 9 and 10); *Bam*HI fragment, 0.341 to 0.346 (lanes 11 and 12); *Bam*HI-*Sst*I fragment, 0.346 to 0.351 (lanes 13 and 14); pSG18-St11, 0.351 to 0.368 (lanes 15 and 16); *Sst*I-*Sal*I fragment, 0.373 to 0.386 (lanes 18 and 19); pSG18-B50-SB160, 0.386 to 0.397 (lanes 20 and 21); pSG18-B53, 0.397 to 0.411 (lanes 22 and 23); pSG18-BE40, 0.411 to 0.421 (lanes 24 and 25); pSG17-EB71, 0.421 to 0.434 (lanes 26 and 27); *Bam*HI-*Kpn*I fragment, 0.435 to 0.438 (lanes 28 and 29); *Kpn*I-*Sal*I fragment, 0.438 to 0.445 (lanes 30 and 31); *Sal*I-*Eco*RI fragment, 0.445 to 0.448 (lanes 32 and 33). Lane 17 shows the migration of the mixed RNA and DNA size standards (see text).

tween 0.309 and 0.351 based on size alone. The continued hybridization of a 5.6-kb mRNA with probes from throughout a 12,000-bp region of the viral genome (0.309 to 0.386) argued in favor of two transcripts of identical size. That two 5.6-kb mRNAs were transcribed was shown by the ability to distinguish them based on their temporal classification and by transcriptional direction studies which showed them to be transcribed from opposite strands (see below).

Plasmid pSG18-BE40 (map coordinates 0.411 to 0.421) and plasmid pSG17-EB71 (0.421 to 0.434) hybridized to mRNA 9 kb in size and to two mRNAs of 4.3 and 4.2 kb, which appeared characteristically as a tight but resolvable doublet (Fig. 2, lanes 25 and 27). Although this 4.2-kb mRNA was indistinguishable in size and temporal class (see below) from the one described above, it was found to be transcribed from the opposite strand of the viral genome (see below). The left end of these transcripts did not appear to extend across the *Bam*HI site at 0.411 (Fig. 2, lanes 23 and 25), but it did span the *Bgl*II site at 0.417 (data not shown). The 9-, 4.3-, and 4.2-kb mRNAs also hybridized to the 450-bp *Bam*HI-*Kpn*I fragment (0.435 to 0.438) (Fig. 2, lane 29) gel purified from a *Kpn*I-*Bam*HI digestion of pSG17. However, only the 9-kb transcript hybridized to the 1,100-bp *Kpn*I-*Sal*I fragment (0.438 to 0.445) (Fig. 2, lane 31) gel purified from a *Kpn*I-*Sal*I-*Eco*RI digestion of pSG17. These two probes also hybridized to mRNAs of 3.0 and 1.4 kb (Fig. 2, lanes 29 and 31). The 450-bp *Sal*I-*Eco*RI fragment (0.445 to 0.448) gel purified from a *Kpn*I-*Sal*I-*Eco*RI digestion of pSG17 hybridized only to the 9- and 3.0-kb mRNAs (Fig. 2, lane 33). These hybridizations indicated that the right end of the 4.3- and 4.2-kb mRNAs and the left end of the 3.0- and 1.4-kb mRNAs were located in the 450-bp region between the *Bam*HI site at 0.435 and the *Kpn*I site at 0.438. The right end of the 1.4-kb mRNA was located between the *Kpn*I site at 0.438 and the *Sal*I site at 0.445. The right end of the 9- and 3.0-kb mRNAs were located beyond the *Eco*RI site at 0.448 (data not shown). The relative position of each transcript described above is summarized (see Fig. 4).

Temporal classification. The ability to detect a specific viral mRNA by Northern hybridization analysis in the RNA extracted from cells before or during viral DNA replication was used to assign a temporal classification to each message. In Fig. 2 the lanes labeled L show the results of hybridization to mRNA isolated from HSV-1-infected cells at 6.5 h postinfection. By this time in the infection cycle, viral DNA synthesis is occurring at maximum rates, and the mRNA population is typical of that seen at late times of infection. However, when the onset of viral DNA synthesis is blocked by maintaining the infected cells in the presence of an inhibitor of viral DNA synthesis, then the mRNA population is typical of that seen at early times of infection (20). In Fig. 2 the lanes labeled E show the results of hybridization to mRNA isolated at 6.5 h postinfection from cells maintained in medium containing 1.9×10^{-4} M 1-β-D-arabinofuranosylthymine. 1-β-D-Arabinofuranosylthymine is an efficient inhibitor of HSV-1 DNA synthesis, and infected cells maintained in its presence contain a viral mRNA population typical of the early phase of the HSV-1 infection cycle (20).

Nine of the transcripts identified and mapped in Fig. 2 showed equal or nearly equal hybridization intensity in both the early and late mRNA samples and were classified as β transcripts. These were the 4.2- and 1.6-kb TK-related mRNAs (Fig. 2, lanes 1 through 4), the 3.3-kb mRNA (lanes 13 through 16), the 5.6-kb mRNA mapping between 0.345 and 0.386 (lanes 13 through 16, 18, and 19), the 4.2-kb mRNA (lanes 18 through 23), the 10-kb mRNA (lanes 13 through 16 and 18 through 23), the 4.3- and 4.2-kb doublet mRNAs (lanes 24 through 29), and the 9-kb mRNA (lanes 24 through 33). Six transcripts were not detected by hybridization to the early mRNA sample, but they hybridized well in the late sample and were classified as γ transcripts. These were the 2.9-kb mRNA mapping downstream from TK (Fig. 2, lanes 1 and 2), the 5.6-, 4.4-, and 2.4-kb mRNAs mapping between 0.309 and 0.351 (lanes 3 through 14), and the 3.0- and 1.4-kb mRNAs mapping to the right of 0.435 (lanes 28 through 33).

Two transcripts appeared to be somewhat intermediate, in that they were detected at low levels in early mRNA but were much more abundant in late mRNA. These were the 5.2- and 1.4-kb mRNAs mapping between 0.315 and 0.351 (Fig. 2, lanes 5 through 14). Transcripts such as these have been classified as βγ transcripts (17, 20).

Experiments have also been done with mRNA isolated from HSV-1-infected cells at 2 and 14 h postinfection (data not shown). Those results were consistent with the temporal classification assigned from the data presented in Fig. 2.

Determination of the direction of transcription. The transcriptional directions were determined by the use of strand-specific hybridization probes. Restriction fragments from a region that would be diagnostic for the mRNAs described above were cloned into the double-stranded replicative form of the filamentous phage cloning vector M13*mp*8 (36). It is always the (+) strand of the M13 phage replicative-form DNA that gets packaged and released as new phage particles. By using purified (+) strand recombinant phage DNA as a template, synthesis of a ^{32}P-labeled (−) strand was initiated at a primer specific for the region 5′ to the M13mp8 cloning sites, so that synthesis of this complementary strand was away from the inserted HSV-1 sequences (25). This (−) strand synthesis was not allowed to proceed to completion; thus, the inserted HSV-1 sequence was kept single stranded. This yielded a partially double-stranded probe that had the hybridization specificity of the inserted, single-stranded HSV-1 sequence. These strand-specific probes were used in hybridization reactions to size fractionated mRNA extracted from cells at 6.5 h postinfection (Fig. 3 and Table 3).

It is standard to designate viral DNA strands as to the direction of their transcription (52). That is, a strand transcribed in the rightward direction is designated *r*, and a strand transcribed in the leftward direction is designated *l*. The *r* strand polarity is 3′ to 5′ from left to right; the *l* strand polarity is 5′ to 3′ from left to right. The polarity, or strand specificity, of the the hybridization probes was identified by determining the orientation of the inserted HSV-1 fragment for each recombinant phage clone from a restriction endonuclease analysis of purified replicative-form DNA (data not shown). Probes made by using *r* strand clones hybridized to mRNAs transcribed in the rightward direction; probes made by using *l* strand clones hybridized to mRNAs transcribed in the leftward direction.

Figure 3 shows the results obtained when six hybridizing probes were used. Clones of the *l* strand of HSV-1 hybridized to the 10- (Fig. 3, lane D and E), 5.6- (lane D), 4.2- (lane E), and 3.3-kb (lane D) mRNAs, which mapped between 0.345 and 0.411, indicating their transcription was in the right-to-left direction. Clones of the *r* strand of HSV-1 hybridized to the 5.6-, 5.2-, 4.4-, and 2.4-kb mRNAs (Fig. 3, lanes A, B, and C), the 1.4-kb mRNA (lanes B and C), which mapped to the left of the *Sst*I site at 0.351, and to the 9-, 4.3-, and 4.2-kb mRNAs (lane F), which mapped to the right of the *Bam*HI site at 0.411. These mRNAs were transcribed in the left-to-right direction. No hybridization was seen when

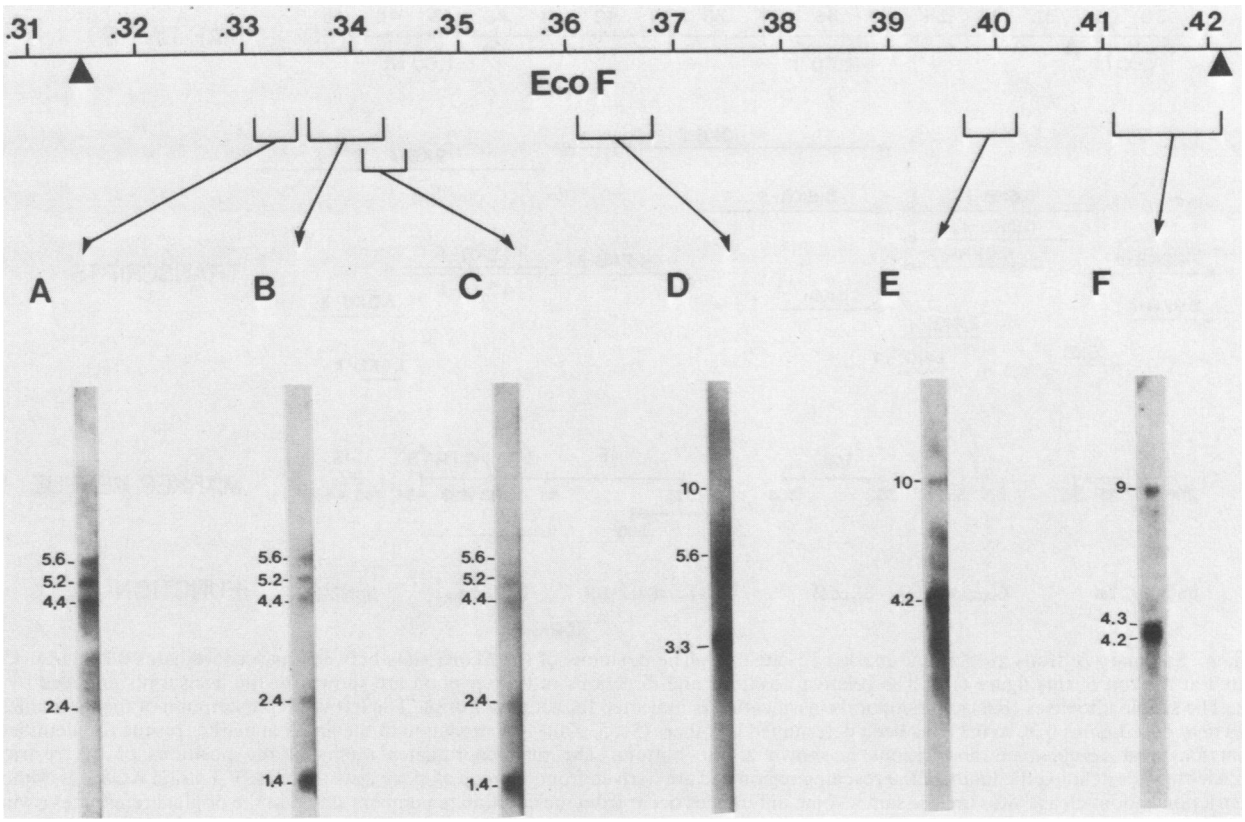

FIG. 3. Results of Northern hybridizations with strand-specific probes. Polyadenylated RNA was isolated from the polyribosomes of cells at 6.5 h postinfection. The RNA was denatured by glyoxalation, size fractionated by agarose gel electrophoresis, and transferred to nitrocellulose paper. ^{32}P-labeled, strand-specific hybridization probes (25) were made by using each of the M13*mp*8 clones listed in Table 3. The sizes in kilobases are shown for the transcripts which hybridized with probes from the indicated regions. Sizes were determined by the migration relative to single-stranded DNA fragments of known size. The map coordinates are indicated within *Eco*RI fragment F relative to the prototype arrangement. The results of hybridizations are shown for clones BS-22 (A), S-3 (B), B-5 (C), SP-4 (D), BS-9 (E), and EB-1 (F).

the other five clones listed in Table 3 were used as probes (data not shown). The hybridization results are summarized in Table 3 and illustrated in Fig. 4.

DISCUSSION

The most striking feature of the transcription pattern summarized in Fig. 4 is the frequency of overlapping transcripts. In his review of HSV transcription, Wagner discusses the common occurrence of overlapping mRNA families encoding the same or different polypeptides, and he suggests four mechanisms involved in generating these families (62). One method involves positioning two promoters near each other, such that the start of translation is downstream from the second promoter. The two mRNAs would thus differ in the length of their 5′-nontranslated leader sequence but would encode the same polypeptide product. A second method involves inefficient transcription termination at a polyadenylation signal. Again, redundant mRNAs would be generated, this time differing in the length of their 3′-nontranslated sequence but still encoding the same polypeptide. Third, overlapping mRNAs are generated when the promoter for one mRNA is located in the interior of another mRNA. Two different, or possibly partially related, polypeptide products would be produced. The fourth mechanism produces overlapping mRNAs by splicing events. The relatedness of the polypeptide products would be dependent on the position of the splice junctions.

The family of five overlapping transcripts between coordinates 0.309 and 0.351 that was identified in this study could be generated from either splicing events, internal promoters, or a combination of the two. Read and Summers (46) and Beck and Millette (4) have identified three rightward promoters active in in vitro transcription systems in the region from 0.310 to 0.320. Two of these are located internally in, but in the opposite direction to, the TK gene. Our hybridization results are consistent with the 5.6-kb transcript originating from one of these two promoters. Wilkie et al. have mapped the 5′ ends of the transcripts spanning the *Bgl*II site at 0.314 (70). Their data suggest that both of these rightward promoters are utilized late (15 h) in infection. The third and rightmost of the in vitro promoters is located between the *Eco*RI site at 0.315 and the *Bam*HI site at 0.320 (4, 46). This is the same region to which we mapped the 5′ end of the 5.2-kb transcript.

The nucleotide sequence of the region around the in vitro promoters (34, 63) shows open reading frames downstream from the three rightward promoters ranging from 13 to 141 codons in length. Unless extensive splicing occurs, this is consistent with a model of internal promoters generating overlapping mRNAs, such that the most 5′ region of each mRNA encodes a unique polypeptide. Therefore, our transcription mapping suggests that five unique, or at most partially related, polypeptide products are encoded by the *r* strand between coordinates 0.309 and 0.351.

The only function known to map in the region from TK to 0.351 is the nucleocapsid structural polypeptide p40. Preston

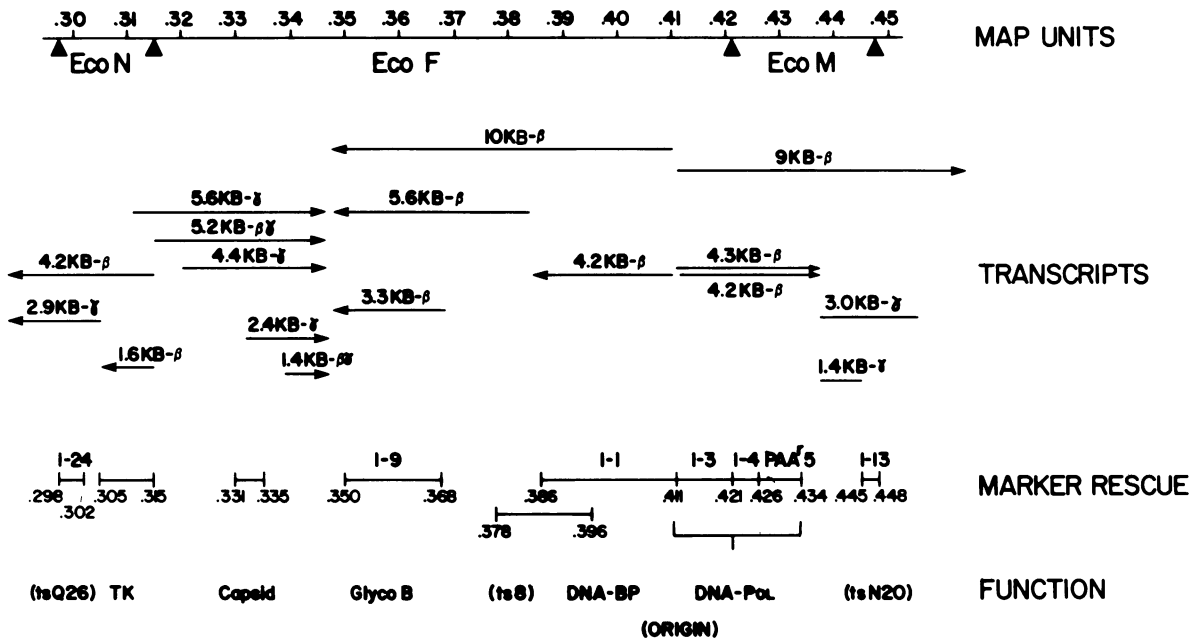

FIG. 4. Summary of transcription and marker rescue data. The positions of the *Eco*RI sites between map coordinates 0.29 and 0.45 are indicated at the top of this figure (19). The relative positions and directions of transcription are shown for the transcripts encoded by this region. The size in kilobases (KB) and temporal classification is indicated for each transcript. The leftward transcription of the three mRNAs located near coordinates 0.30 to 0.31 has been determined by others (51, 53, 70). A compilation of the limits of marker rescue for identified viral functions and complementation groups is shown at the bottom. The map coordinates represent the positions of the restriction endonuclease sites defining the limits of the rescuing region and are derived from our map of cleavage sites in HSV-1 strain KOS 1.1. Although the restriction endonuclease sites are the same, some differences occur from the coordinate numbers stated in the original references owing to normalization to our restriction map. The mapping of the *ts*Q26 mutation in complementation group 1-24 is from reference 66; mapping of TK is from references 34 and 63; mapping of the capsid protein p40 mutation is from reference 42; mapping of glycoprotein B mutations is from references 14, 23, and 30; mapping of the *ts*8 mutation is reported here (see text); mapping of DNA-binding protein mutations in complementation group 1-1 is from references 10, 29, and 67, and this report (see text); the location of the origin of viral DNA synthesis is from references 16 and 55; mapping of mutations in the DNA polymerase gene is from references 7–9 and this report (see text); mapping of the *ts*N20 mutation in complementation group 1-13 is from reference 9.

et al. have mapped a *ts* lesion in this protein to the region between the *Sal*I site at 0.331 and the *Bam*HI site at 0.335 by marker rescue (42). This region is not contained in the 1.4-kb mRNA, but represents the 5′ half of the 2.4-kb mRNA. Since the region of rescue is located in the 3′ half of the 5.6-, 5.2-, and 4.4-kb mRNAs and since the gene size predicted for a polypeptide of molecular weight 38,000 to 45,000 is less than 1.5 kb, it is likely that the 2.4-kb mRNA encodes the nucleocapsid polypeptide designated p40.

Bzik and Person (personal communication) have identified by sequence and RNA mapping analysis a promoter just to the right of the *Xho*I site at coordinate 0.368. This represents a promoter for the 3.3-kb mRNA, which is internal in both the 5.6- and 10-kb mRNAs. Their nucleotide sequence identifies termination signals upstream from the promoter for the 3.3-kb mRNA in all three reading frames. Thus, the 5.6- and 3.3-kb mRNAs would each be expected to encode a unique polypeptide.

Marker rescue experiments have localized mutations in the gene for glycoprotein B (group 1-9) to the region 0.346 to 0.368 (14, 23, 30). De Luca et al. have mapped three mutations associated with glycoprotein B to separate positions within this region (14). Holland et al. have isolated viruses containing antigenic variations of the glycoproteins by selecting for viruses resistant to neutralization by monoclonal antibodies (22). One of these variants (*mar*B1.1), resistant to neutralization by a monoclonal antibody to glycoprotein B, is rescued to wild-type glycoprotein B antigenicity by the region 0.351 to 0.361 (23).

Map coordinates 0.346 to 0.368 correspond to the region to which we have mapped the 3.3-kb mRNA (Fig. 4). Cleveland and Millette (personal communication) and Rafield and Knipe (45) have isolated mRNA from this region by hybridization selection and translated it in vitro. Both groups find a polypeptide which is immunoprecipitated with monoclonal antibodies to glycoprotein B. This, along with the sequence and marker rescue data, indicates that the 3.3-kb mRNA encodes glycoprotein B.

The mutants *ts*8 and *ts*17 appear to represent a new HSV-1 complementation group (Table 2). Mutant *ts*8, which we incorrectly reported to have a DNA-negative phenotype (18), and mutant *ts*17 both synthesize normal amounts of viral DNA at the nonpermissive temperature (39°C). Mutant *ts*8 has previously been shown to synthesize wild-type levels of virus-specific glycoproteins and shows no appreciable difference in the banding pattern of ^{35}S-labeled infected cell polypeptides (18). Although these phenotypes suggest that the mutation is in a late viral gene, marker rescue mapping associates it with a region of β transcripts (Fig. 4). Since these two mutants complement all of our group 1-1 and 1-9 mutants, they may represent the viral gene encoded by the 5.6-kb mRNA. This is similar to the situation with the group 1-9 mutants. They have a DNA-positive phenotype (Table 2; 50), yet the gene they define (glycoprotein B) is expressed as an early (β-class) 3.3-kb mRNA. Mutants *ts*8 and *ts*17 may similarly represent a viral gene product made at early times, but not involved in viral DNA synthesis.

Pancake et al. recently reported the isolation of a class of

mutants selected for resistance to immune cytolysis (38). One of these mutants (*icr ts*78) has a DNA-positive phenotype and synthesizes wild-type levels of the glycoproteins, but expresses the glycoproteins in reduced amounts on the surface of infected cells. The mutation of *icr ts*78 mapped by marker rescue to both *Eco*RI fragment F (map coordinates 0.315 to 0.421) and the portion of the long unique segment contained in *Xba*I fragment G (0.058 to 0.074). This mutant complemented several HSV-1 mutants, but failed to complement two mutants in a newly identified HSV-2 gene. This led Pancake et al. to suggest that *icr ts*78 represents the HSV-1 equivalent of this HSV-2 gene, which maps between the genes for glycoprotein B and DNA-binding protein (15, 56), and to define a new HSV-1 cistron designated 1-33 (38). Mutant *ts*8 resembles mutant *icr ts*78 in that it has a DNA-positive phenotype and synthesizes wild-type glycoprotein levels. However, in contrast to mutant *icr ts*78, mutant *ts*8 expresses normal amounts of cell surface glycoproteins and is sensitive to immune cytolysis (18). Another difference is that the mutation of *ts*8 was rescued only by sequences within *Eco*RI fragment F (0.378 to 0.397), which are comparable to the location of the HSV-2 mutations (15, 56), and not by sequences from the region 0.058 to 0.074. Complementation tests of mutants *ts*8 and *ts*17 with mutant *icr ts*78 (38) and the HSV-2 mutants *ts*39 and *ts*201 (15) are needed to determine whether all five mutations represent the same viral function.

The 10- and 4.2-kb mRNAs would be expected to encode the same polypeptide, since the sequences of the 4.2-kb mRNA represent the most 5′ sequences of the 10-kb mRNA. Whether the 10-kb mRNA represents a primary transcript that is then inefficiently processed to give a 4.2-kb mRNA or a transcript resulting from read-through by inefficient termination at a polyadenylation signal has not been determined. From the limits of marker rescue which define complementation group 1-1 (Fig. 4; 10, 29, 67), we suggest that the 10- and 4.2-kb mRNAs encode the major DNA-binding protein. Cleveland and Millette (personal communication) and Rafield and Knipe (45) have also isolated mRNA from this region by hybrid selection and found that it encodes a polypeptide having a molecular weight of ca. 130,000. The major message selected is 4.2 to 4.5 kb in size, and the translation product is immunoprecipitated with monoclonal antibodies to the DNA-binding protein (45).

Two transcripts, differing in size by less than 100 nucleotides, were mapped to the region 0.411 to 0.438. These two mRNAs are most likely generated by either a splicing event or by two closely spaced promoters. They also contain the same information as the 5′ half of the 9-kb transcript. We could not resolve whether two transcripts of ca. 9 kb were present, but it is likely that this larger transcript is related to the 4.3- and 4.2-kb mRNAs by an inefficient termination at the polyadenylation signal utilized by the 4.3- and 4.2-kb mRNAs.

The region spanning the *Eco*RI site at 0.421 has been associated with the HSV-1-specified DNA polymerase (7, 8, 12, 13, 27). Complementation groups 1-3 and 1-4, both characterized as specifying a thermolabile DNA polymerase (3, 43, 44), have been mapped to this region (Table 2 and Fig. 4; 7, 9, 39). Also, mutations resulting in the resistance of the viral DNA polymerase to the DNA synthesis inhibitor phosphonoacetic acid have been mapped to this region (7–9). Thus, the 4.3-kb mRNA or the 4.2-kb mRNA or possibly both is a likely candidate to encode the HSV-1 DNA polymerase.

Kudler et al. (28) have performed a heteroduplex analysis of the homology between cloned fragments of HSV type 1 and HSV type 2. When they examined heteroduplexes between the *Eco*RI fragment F from HSV-1 and the corresponding colinear region of HSV-2, they observed four regions of good homology separated by three regions of at least partial nonhomology. Although they were unable to define the left and right ends, one of the two possible alignments would be consistent with regions of nonhomology located around coordinates 0.350, 0.380, and 0.410. Our transcription map predicts these three areas to contain sequences involved in promotion (0.410) or termination (0.350) of transcription or both (0.380).

A correlation can also be made for transcripts associated with two more complementation groups. Sharp et al. (51) have described a 3.1-kb late mRNA mapping just downstream from TK and an overlapping minor transcript of 4.8 kb associated with it. Our mapping of a 2.9-kb late mRNA and an overlapping 4.2-kb early mRNA supports their findings, with a slight difference in size assignment. Weller et al. (66) have recently mapped a *ts* mutation (*ts*Q26) in a putatively late viral function to the region just to the left of TK. This mutant, which defines complementation group 1-24, probably represents the viral gene encoded by the 2.9-kb mRNA. The mutation for *ts*N20 (complementation group 1-13) in another late viral gene (66) has been mapped by Coen et al. (9) by marker rescue to the 450-bp *Sal*I-*Eco*RI fragment (0.445 to 0.448) located at the right end of *Eco*RI fragment M. This mutation should define the viral gene encoded by the 3.0-kb late mRNA since the 1.4-kb late mRNA mapped to the left of this region.

We infer from transcriptional analysis that 13 viral genes are represented in the 23,000-bp region defined by *Eco*RI fragments N, F, and M (coordinates 0.298 to 0.448). Functions or mutations or both are known for eight of these genes. Polypeptides involved and required for viral DNA synthesis as well as polypeptides serving structural roles are encoded within this region. It is also interesting to note that one of the putative origins for viral DNA replication suggested by Frenkel and co-workers (16, 55) would seem to be located near the 5′ end of both the gene encoding the major DNA-binding protein and the gene encoding the DNA polymerase. The control of viral DNA synthesis relative to the regulation of expression for these genes should prove to be very interesting. This 23,000-bp region has also been implicated in morphological transformation (5, 47). Although our analysis detects no obvious candidates for the gene or genes responsible for this, it does define the limits of the major viral genes and suggests regions for attack by in vitro mutagenesis for elucidating other viral functions.

ACKNOWLEDGMENTS

We thank David Knipe, John Cleveland, Bob Millette, Sandra Weller, Priscilla Schaffer, Don Coen, David Bzik, Stan Person, and Ed Wagner for communicating results before publication. Discussions with Ed Wagner and Fred Homa are also appreciated. We thank Bill Folk, Bill Farmerie, and Steve Triezenberg for helpful suggestions and for kindly supplying starter cultures for M13 cloning.

This work was supported by Public Health Service grants AI 17900, AI 18228, and RR 00200 from the National Institutes of Health. L.E.H. was supported by National Institutes of Health postdoctoral training grant T32-CA09281; A.L.G. was supported by Medical Scientist Training Program grant GM 07863.

LITERATURE CITED

1. **Adler, R., J. C. Glorioso, and M. Levine.** 1978. Infection by herpes simplex virus and cells of nervous system origin: charac-

terization of a non-permissive interaction. J. Gen. Virol. **39**:9–20.
2. **Anderson, K. P., J. R. Stringer, L. E. Holland, and E. K. Wagner.** 1979. Isolation and localization of herpes simplex virus type 1 mRNA. J. Virol. **30**:805–820.
3. **Aron, G. M., D. J. M. Purifoy, and P. A. Schaffer.** 1975. DNA synthesis and DNA polymerase activity of herpes simplex virus type 1 temperature-sensitive mutants. J. Virol. **16**:498–507.
4. **Beck, T. W., and R. L. Millette.** 1982. Regulation of herpes simplex virus gene transcription *in vitro*. J. Cell. Biochem. **19**:333–347.
5. **Camacho, A., and P. G. Spear.** 1978. Transformation of hamster embryo fibroblasts by a specific fragment of the herpes simplex virus genome. Cell **15**:993–1002.
6. **Carmichael, G. G., and G. K. McMaster.** 1980. The analysis of nucleic acids in gels using glyoxal and acridine orange. Methods Enzymol. **65**:380–391.
7. **Chartrand, P., C. S. Crumpacker, P. A. Schaffer, and N. M. Wilkie.** 1980. Physical and genetic analysis of the herpes simplex virus DNA polymerase locus. Virology **103**:311–326.
8. **Chartrand, P., N. D. Stow, M. C. Timbury, and N. M. Wilkie.** 1979. Physical mapping of *paa*^{r} mutations of herpes simplex virus type 1 and type 2 by intertypic marker rescue. J. Virol. **31**:265–276.
9. **Coen, D. M., D. P. Aschman, P. T. Gelep, M. J. Retondo, S. K. Weller, and P. A. Schaffer.** 1984. Fine mapping and molecular cloning of mutations in the herpes simplex virus DNA polymerase locus. J. Virol. **49**:236–247.
10. **Conley, A. J., D. M. Knipe, P. C. Jones, and B. Roizman.** 1981. Molecular genetics of herpes simplex virus. VII. Characterization of a temperature-sensitive mutant produced by in vitro mutagenesis and defective in DNA synthesis and accumulation of γ polypeptides. J. Virol. **37**:191–206.
11. **Cremer, K., M. Bodemer, and W. C. Summers.** 1978. Characterization of the mRNA for herpes simplex virus thymidine kinase by cell-free synthesis of active enzyme. Nucleic Acids Res. **5**:2333–2344.
12. **Crumpacker, C. S., P. Chartrand, J. H. Subak-Sharpe, and N. M. Wilkie.** 1980. Resistance of herpes simplex virus to acycloguanosine—genetic and physical analysis. Virology **105**:171–184.
13. **Crumpacker, C. S., L. E. Schnipper, P. N. Kowalsky, and D. M. Sherman.** 1982. Resistance of herpes simplex virus to adenine arabinoside and E-5-(2-bromovinyl)-2′-deoxyuridine: a physical analysis. J. Infect. Dis. **146**:167–172.
14. **DeLuca, N., D. J. Bzik, V. C. Bond, S. Person, and W. Snipes.** 1982. Nucleotide sequences of herpes simplex virus type 1 (HSV-1) affecting virus entry, cell fusion, and production of glycoprotein gB (VP7). Virology **122**:411–423.
15. **Dixon, R. A. F., D. J. Sabourin, and P. A. Schaffer.** 1983. Genetic analysis of temperature-sensitive mutants which define the genes for the major herpes simplex virus type 2 DNA-binding protein and a new late function. J. Virol. **45**:343–353.
16. **Frenkel, N., H. Locker, and D. A. Vlazny.** 1980. Studies of defective herpes simplex viruses. Ann. N.Y. Acad. Sci. **354**:347–370.
17. **Frink, R. J., K. P. Anderson, and E. K. Wagner.** 1981. Herpes simplex virus type 1 *Hin*dIII fragment L encodes spliced and complementary mRNA species. J. Virol. **39**:559–572.
18. **Glorioso, J. C., M. Levine, T. C. Holland, and M. S. Szczesiul.** 1980. Mutant analysis of herpes simplex virus-induced cell surface antigens: resistance to complement-mediated immune cytolysis. J. Virol. **35**:672–681.
19. **Goldin, A. L., R. M. Sandri-Goldin, M. Levine, and J. C. Glorioso.** 1981. Cloning of herpes simplex virus type 1 sequences representing the whole genome. J. Virol. **38**:50–58.
20. **Holland, L. E., K. P. Anderson, C. Shipman, Jr., and E. K. Wagner.** 1980. Viral DNA synthesis is required for the efficient expression of specific herpes simplex virus type 1 mRNA species. Virology **101**:10–24.
21. **Holland, L. E., K. P. Anderson, J. R. Stringer, and E. K. Wagner.** 1979. Isolation and localization of herpes simplex virus type 1 mRNA abundant before viral DNA synthesis. J. Virol. **31**:447–462.
22. **Holland, T. C., S. D. Marlin, M. Levine, and J. Glorioso.** 1983. Antigenic variants of herpes simplex virus selected with glycoprotein-specific monoclonal antibodies. J. Virol. **45**:672–682.
23. **Holland, T. C., R. M. Sandri-Goldin, L. E. Holland, S. D. Marlin, M. Levine, and J. C. Glorioso.** 1983. Physical mapping of the mutation in an antigenic variant of herpes simplex virus type 1 by use of an immunoreactive plaque assay. J. Virol. **46**:649–652.
24. **Holmes, D. S., and M. Quigley.** 1981. A rapid boiling method for the preparation of bacterial plasmids. Anal. Biochem. **114**:193–197.
25. **Hu, N. T., and J. Messing.** 1982. The making of strand-specific M13 probes. Gene **17**:271–277.
26. **Hughes, R. G., Jr., and W. H. Munyon.** 1975. Temperature-sensitive mutants of herpes simplex virus type 1 defective in lysis but not in transformation. J. Virol. **16**:275–283.
27. **Knopf, K. W., E. R. Kaufman, and C. Crumpacker.** 1981. Physical mapping of drug resistance mutations defines an active center of the herpes simplex virus DNA polymerase enzyme. J. Virol. **39**:746–757.
28. **Kudler, L., T. R. Jones, R. J. Russell, and R. W. Hyman.** 1983. Heteroduplex analysis of cloned fragments of herpes simplex virus DNAs. Virology **124**:86–99.
29. **Lee, C. K., and D. M. Knipe.** 1983. Thermolabile in vivo DNA-binding activity associated with a protein encoded by mutants of herpes simplex virus type 1. J. Virol. **46**:909–919.
30. **Little, S. P., J. T. Jofre, R. J. Courtney, and P. A. Schaffer.** 1981. A virion-associated glycoprotein essential for infectivity of herpes simplex virus type 1. Virology **115**:149–160.
31. **Maniatis, T., E. F. Fritsch, and J. Sambrook.** 1982. Molecular cloning, p. 88–89. Cold Spring Harbor Laboratory, Cold Spring Harbor, N.Y.
32. **Maniatis, T., A. Jeffrey, and H. van deSande.** 1975. Chain length determination of small double and single-stranded DNA molecules by polyacrylamide gel electrophoresis. Biochemistry **14**:3787–3794.
33. **Manservigi, R., P. G. Spear, and A. Buchan.** 1977. Cell fusion induced by herpes simplex virus is promoted and suppressed by different viral glycoproteins. Proc. Natl. Acad. Sci. U.S.A. **74**:3913–3917.
34. **McKnight, S. L.** 1980. The nucleotide sequence and transcript map of the herpes simplex virus thymidine kinase gene. Nucleic Acids Res. **8**:5949–5964.
35. **McMaster, G. K., and G. G. Carmichael.** 1977. Analysis of single- and double-stranded nucleic acids on polyacrylamide and agarose gels by using glyoxal and acridine orange. Proc. Natl. Acad. Sci. U.S.A. **74**:4835–4838.
36. **Messing, J., and J. Vieira.** 1982. A new pair of M13 vectors for selecting either DNA strand of double-digest restriction fragments. Gene **19**:269–276.
37. **Palmiter, R. D.** 1974. Magnesium precipitation of ribonucleoprotein complexes. Expedient techniques for the isolation of undegraded polysomes and messenger ribonucleic acid. Biochemistry **13**:3606–3614.
38. **Pancake, B. A., D. P. Aschman, and P. A. Schaffer.** 1983. Genetic and phenotypic analysis of herpes simplex virus type 1 mutants conditionally resistant to immune cytolysis. J. Virol. **47**:568–585.
39. **Parris, D. S., R. A. F. Dixon, and P. A. Schaffer.** 1980. Physical mapping of herpes simplex virus type 1 ts mutants by marker rescue: correlation of the physical and genetic maps. Virology **100**:275–287.
40. **Post, L. E., A. J. Conley, E. S. Mocarski, and B. Roizman.** 1980. Cloning of reiterated and nonreiterated herpes simplex virus 1 sequences as BamHI fragments. Proc. Natl. Acad. Sci. U.S.A. **77**:4201–4205.
41. **Prentki, P., F. Karch, S. Iida, and J. Meyer.** 1981. The plasmid cloning vector pBR325 contains a 482 base-pair-long inverted duplication. Gene **14**:289–299.
42. **Preston, V. G., J. A. V. Coates, and F. J. Rixon.** 1983. Identification and characterization of a herpes simplex virus gene product required for encapsidation of virus DNA. J. Virol. **45**:1056–1064.
43. **Purifoy, D. J. M., R. B. Lewis, and K. L. Powell.** 1977. Identifi-

cation of the herpes simplex virus DNA polymerase gene. Nature (London) **269**:621–623.
44. **Purifoy, D. J. M., and K. L. Powell.** 1981. Temperature-sensitive mutants in two distinct complementation groups of herpes simplex virus type 1 specify thermolabile DNA polymerase. J. Gen. Virol. **54**:219–222.
45. **Rafield, L. F., and D. M. Knipe.** 1984. Characterization of the major mRNAs transcribed from the genes for glycoprotein B and DNA-binding protein ICP8 of herpes simplex virus type 1. J. Virol. **49**:960–969.
46. **Read, G. S., and W. C. Summers.** 1982. *In vitro* transcription of the thymidine kinase gene of herpes simplex virus. Proc. Natl. Acad. Sci. U.S.A. **79**:5215–5219.
47. **Reyes, G. R., R. LaFemina, S. D. Hayward, and G. S. Hayward.** 1980. Morphological transformation by DNA fragments of human herpesviruses: evidence for two distinct transforming regions in herpes simplex virus types 1 and 2 and lack of correlation with biochemical transfer of the thymidine kinase gene. Cold Spring Harbor Symp. Quant. Biol. **44**:629–641.
48. **Sandri-Goldin, R. M., A. L. Goldin, L. E. Holland, J. C. Glorioso, and M. Levine.** 1983. Expression of herpes simplex virus β and γ genes integrated in mammalian cells and their induction by an α gene product. Mol. Cell. Biol. **3**:2028–2044.
49. **Sandri-Goldin, R. M., M. Levine, and J. C. Glorioso.** 1981. Method for induction of mutations in physically defined regions of the herpes simplex virus genome. J. Virol. **38**:41–49.
50. **Schaffer, P. A., V. C. Carter, and M. C. Timbury.** 1978. Collaborative complementation study of temperature-sensitive mutants of herpes simplex virus types 1 and 2. J. Virol. **27**:490–504.
51. **Sharp, J. A., M. J. Wagner, and W. C. Summers.** 1983. Transcription of herpes simplex virus genes in vivo: overlap of a late promoter with the 3′ end of the early thymidine kinase gene. J. Virol. **45**:10–17.
52. **Sharp, P. A., P. H. Gallimore, and S. J. Flint.** 1974. Mapping of adenovirus 2 RNA sequences in lytically infected cells and transformed cell lines. Cold Spring Harbor Symp. Quant. Biol. **39**:457–474.
53. **Smiley, J. R., M. J. Wagner, W. P. Summers, and W. C. Summers.** 1980. Genetic and physical evidence for the polarity of transcription of the thymidine kinase gene of herpes simplex virus. Virology **102**:83–93.
54. **Southern, E. M.** 1975. Detection of specific sequences among DNA fragments separated by gel electrophoresis. J. Mol. Biol. **98**:503–533.
55. **Spaete, R. R., and N. Frenkel.** 1982. The herpes simplex virus amplicon: a new eucaryotic defective-virus cloning-amplifying vector. Cell **30**:295–304.
56. **Spang, A. E., P. J. Godowski, and D. M. Knipe.** 1983. Characterization of herpes simplex virus 2 temperature-sensitive mutants whose lesions map in or near the coding sequences for the major DNA-binding protein. J. Virol. **45**:332–342.
57. **Spear, P. G., and B. Roizman.** 1980. Herpes simplex viruses, p. 615–745. *In* J. Tooze (ed.), DNA tumor viruses. Cold Spring Harbor Laboratory, Cold Spring Harbor, N.Y.
58. **Stringer, J. R., L. E. Holland, R. I. Swanstrom, K. Pivo, and E. K. Wagner.** 1977. Quantitation of herpes simplex virus type 1 RNA in infected HeLa cells. J. Virol. **21**:889–901.
59. **Sutcliffe, J. G.** 1978. pBR322 restriction map derived from the DNA sequence: accurate DNA size markers up to 4361 nucleotide pairs long. Nucleic Acids Res. **5**:2721–2728.
60. **Thomas, P. S.** 1980. Hybridization of denatured RNA and small DNA fragments transferred to nitrocellulose. Proc. Natl. Acad. Sci. U.S.A. **77**:5201–5205.
61. **Villa-Komaroff, L., A. Efstratiadis, S. Broome, P. Lomedico, R. Tizard, S. P. Naber, W. L. Chick, and W. Gilbert.** 1978. A bacterial clone synthesizing proinsulin. Proc. Natl. Acad. Sci. U.S.A. **75**:3727–3731.
62. **Wagner, E. K.** 1983. Transcription patterns in HSV infections. Adv. Viral Oncol. **3**:239–270.
63. **Wagner, M. J., J. A. Sharp, and W. C. Summers.** 1981. Nucleotide sequence of the thymidine kinase gene of herpes simplex virus type 1. Proc. Natl. Acad. Sci. U.S.A. **78**:1441–1445.
64. **Weissbach, A., S. L. Hong, J. Aucker, and R. Muller.** 1973. Characterization of herpes simplex virus-induced deoxyribonucleic acid polymerase. J. Biol. Chem. **248**:6270–6277.
65. **Wellauer, P. K., and I. B. Dawid.** 1973. Secondary structure maps of RNA: processing of HeLa ribosomal RNA. Proc. Natl. Acad. Sci. U.S.A. **70**:2827–2831.
66. **Weller, S. K., D. P. Aschman, W. R. Sacks, D. M. Coen, and P. A. Schaffer.** 1983. Genetic analysis of temperature-sensitive mutants of HSV-1: the combined use of complementation and physical mapping for cistron assignment. Virology **130**:290–305.
67. **Weller, S. K., K. J. Lee, D. J. Sabourin, and P. A. Schaffer.** 1983. Genetic analysis of temperature-sensitive mutants which define the gene for the major herpes simplex virus type 1 DNA-binding protein. J. Virol. **45**:354–366.
68. **Wigler, M., A. Pellicer, S. Silverstein, R. Axel, G. Urlaub, and L. Chasin.** 1979. DNA-mediated transfer of the adenine phosphoribosyltransferase locus into mammalian cells. Proc. Natl. Acad. Sci. U.S.A. **76**:1373–1376.
69. **Wigler, M., S. Silverstein, L.-S. Lee, A. Pellicer, Y. Cheng, and R. Axel.** 1977. Transfer of purified herpes virus thymidine kinase gene to cultured mouse cells. Cell **11**:223–232.
70. **Wilkie, N. M., R. P. Eglin, P. G. Sanders, and J. B. Clements.** 1980. The association of herpes simplex virus with squamous carcinoma of the cervix, and studies of the virus thymidine kinase gene. Proc. R. Soc. Lond. Ser. B **210**:411–421.